

Off-equilibrium scaling behaviors driven by time-dependent external fields in three-dimensional $O(N)$ vector models

Andrea Pelissetto¹ and Ettore Vicari²

¹ *Dipartimento di Fisica dell'Università di Roma "La Sapienza" and INFN, Sezione di Roma I, I-00185 Roma, Italy and*

² *Dipartimento di Fisica dell'Università di Pisa and INFN, Largo Pontecorvo 3, I-56127 Pisa, Italy*

(Dated: June 21, 2021)

We consider the dynamical off-equilibrium behavior of the three-dimensional $O(N)$ vector model in the presence of a slowly-varying time-dependent spatially-uniform magnetic field $\mathbf{H}(t) = h(t) \mathbf{e}$, where \mathbf{e} is a N -dimensional constant unit vector, $h(t) = t/t_s$, and t_s is a time scale, at fixed temperature $T \leq T_c$, where T_c corresponds to the continuous order-disorder transition. The dynamic evolutions start from equilibrium configurations at $h_i < 0$, correspondingly $t_i < 0$, and end at time $t_f > 0$ with $h(t_f) > 0$, or vice versa. We show that the magnetization displays an off-equilibrium scaling behavior close to the transition line $\mathbf{H}(t) = 0$. It arises from the interplay among the time t , the time scale t_s , and the finite size L . The scaling behavior can be parametrized in terms of the scaling variables t_s^κ/L and $t/t_s^{\kappa_t}$, where $\kappa > 0$ and $\kappa_t > 0$ are appropriate universal exponents, which differ at the critical point and for $T < T_c$. In the latter case, κ and κ_t also depend on the shape of the lattice and on the boundary conditions. We present numerical results for the Heisenberg ($N = 3$) model under a purely relaxational dynamics. They confirm the predicted off-equilibrium scaling behaviors at and below T_c . We also discuss hysteresis phenomena in round-trip protocols for the time dependence of the external field. We define a scaling function for the hysteresis loop area of the magnetization that can be used to quantify how far the system is from equilibrium.

PACS numbers: 64.70.qj, 64.60.Ht, 64.60.an

I. INTRODUCTION

Statistical systems show notable off-equilibrium behaviors at phase transitions. For example, metastability and hysteresis phenomena occur at first-order transitions [1], while the Kibble-Zurek (KZ) mechanism [2, 3] is observed at continuous transitions. They may arise when one of the model parameters, such as the temperature or the external magnetic field in spin systems, varies across the transition point with a time scale t_s . In this case some large-scale modes do not equilibrate, even in the limit of large t_s , giving rise to peculiar off-equilibrium behaviors. These phenomena are of great interest in many different physical contexts, see, e.g., Refs. [1–7].

Off-equilibrium phenomena due to the inability of the system to adapt itself to changes of the external parameters have been much investigated at continuous transitions. As it happens for the equilibrium static and dynamic critical behavior, off-equilibrium behaviors driven by slow changes of external parameters show universal features. For $t_s \rightarrow \infty$ and close to the transition point, one can define general scaling expressions in terms of the standard critical exponents characterizing the statics and dynamics of the system at equilibrium [2, 3, 6, 8, 9]. A prototypical example is the KZ mechanism [2, 3] for the formation of topological defects when the temperature is slowly changed across a continuous transition, from the disordered to the ordered phase. In this case, if T_c is the critical temperature, one considers the protocol $T(t)/T_c = 1 - t/t_s$ starting from $t = t_i < 0$ to $t = t_f > 0$, where t_s controls the speed of the temperature variation. In the large- t_s limit, the system shows off-equilibrium scaling behaviors across the transition [3, 9]. Analogous

phenomena are expected at quantum transitions, when the system is driven across a continuous transition by quasi-adiabatic changes of external parameters [5, 10–13]. Many experiments have addressed the same issues in several different physical systems [14–36]. We mention, as an example, the recent studies characterizing the dynamic formation of Bose-Einstein condensates, see, e.g., Ref. [7] and references therein.

In this paper we consider off-equilibrium phenomena driven by slowly-varying external fields coupled to the order parameter at finite-temperature phase transitions, in systems characterized by a continuous $O(N)$ symmetry. In particular, we study the off-equilibrium behavior of the three-dimensional (3D) $O(N)$ vector model at fixed temperature T in the presence of a slowly-varying time-dependent spatially-uniform external field coupled to the vector order parameter. We consider a *magnetic* field $\mathbf{H}(t) = h(t)\mathbf{e}$ with fixed direction \mathbf{e} and time-dependent amplitude $h(t) = t/t_s$, where t_s is a time scale. In the high-temperature paramagnetic phase, in which the correlation length is finite in the infinite-volume limit, the system always reaches equilibrium for sufficiently large time scales t_s . Instead, at the critical point T_c , infinite-volume systems are unable to equilibrate for $t \approx 0$, when the magnetic field crosses the transition point $h = 0$, even in the large- t_s limit. The off-equilibrium behavior close to the transition point turns out to be universal. Its general features can be derived by using scaling arguments analogous to those leading to the KZ mechanism [8, 9].

Our main results concern the extension of these off-equilibrium studies to the low-temperature $T < T_c$ phase, where a spatially-uniform magnetic field drives first-order transitions: the magnetization has a discontinuity at the

transition point $\mathbf{H} = 0$ in the thermodynamic limit. As expected, equilibration becomes significantly harder across first-order transitions. However, we show that slow variations of the magnetic field give rise to universal off-equilibrium scaling behaviors also across this class of first-order transitions, as in the continuous case. General scaling predictions can be derived by combining the KZ arguments with the general results for the equilibrium static and dynamic behaviors of finite-size systems at first-order transitions.

Therefore, for any $T \leq T_c$, and for $t \approx 0$ corresponding to $h(t) \approx 0$, the dynamics of the system is expected to show a universal off-equilibrium scaling behavior, which arises from the interplay among the time t , the time scale t_s , and the size L of the system. In this regime the time dependence of the magnetization can be expressed in terms of scaling functions that depend on the scaling variables t_s^κ/L and $t/t_s^{\kappa_t}$, where $\kappa > 0$ and $\kappa_t > 0$ are appropriate universal exponents, which differ at the critical point and for $T < T_c$. In the latter case, κ and κ_t also depend on the shape of the lattice and on the boundary conditions. In order to check the general scaling theory, we present a numerical analysis of the 3D Heisenberg ($N = 3$) model both for $T = T_c$ and for a few values of $T < T_c$. In our Monte Carlo (MC) simulations we consider a purely relaxational dynamics.

We also extend our study to round-trip protocols, in which the magnetic-field amplitude $h(t)$ is varied between $h_i < 0$ and $h_f > 0$ and then back again to $h_i < 0$. In this case we observe off-equilibrium hysteresis phenomena at the critical point T_c and below T_c , which are characterized in terms of appropriate scaling functions.

The paper is organized as follows. In Sec. II we put forward the general scaling theory appropriate to describe the off-equilibrium phenomena occurring in the $O(N)$ vector model in the presence of a slowly-varying magnetic field, both for $T = T_c$ and $T < T_c$. Sec. III discusses some features of the equilibrium static and dynamic finite-size scaling of the $O(N)$ vector model in the low-temperature phase $T < T_c$ and at T_c . The corresponding critical exponents allow us to determine the appropriate scaling variables that parametrize the off-equilibrium behavior of the magnetization. In Sec. IV we check the scaling arguments by numerical simulations of the 3D Heisenberg lattice model under a relaxational dynamics. We show that the magnetization displays the predicted scaling behavior along the low-temperature first-order transition line ($T < T_c$) and at the critical point T_c . In Sec. V we discuss the hysteresis phenomena that occur in round-trip protocols, in which the external field is first increased from $h_i < 0$ to $h_f > 0$ and then decreased again to h_i . We determine the scaling behavior of the area enclosed by the hysteresis loop of the magnetization at and below T_c . Finally, in Sec. VI we draw some conclusions.

II. OFF-EQUILIBRIUM SCALING DRIVEN BY MAGNETIC FIELDS

A. The 3D $O(N)$ vector model

We study the 3D $O(N)$ vector model in the presence of a uniform magnetic field. We consider N -component unit-length spins \mathbf{s}_i , defined on a simple cubic lattice, and the Hamiltonian

$$\mathcal{H} = -J \sum_{\langle ij \rangle} \mathbf{s}_i \cdot \mathbf{s}_j - \mathbf{H} \cdot \sum_i \mathbf{s}_i, \quad (1)$$

where $\langle ij \rangle$ indicates nearest-neighbor sites and $J > 0$. In the following we set $J = 1$, so that all energies are expressed in units of J . We write the magnetic field as

$$\mathbf{H} = h\mathbf{e}, \quad \mathbf{e} \cdot \mathbf{e} = 1. \quad (2)$$

We consider cubic ($L \times L \times L$) and anisotropic cylinder-like ($L \times L \times L_{\parallel}$ with $L_{\parallel} \propto L^2$) systems, with periodic boundary conditions (PBC) along all directions.

In the absence of an external magnetic field, i.e., for $\mathbf{H} = 0$, the system undergoes a continuous transition at a finite temperature T_c , which separates the high-temperature paramagnetic phase from the low-temperature ferromagnetic phase. In the low-temperature phase $T < T_c$, the external magnetic field drives first-order transitions at $h = 0$, giving rise to a discontinuity in the magnetization. We have

$$\lim_{h \rightarrow \pm 0} \lim_{L \rightarrow \infty} m(L, h, T) = \pm m_0(T), \quad (3)$$

where

$$m \equiv \mathbf{M} \cdot \mathbf{e}, \quad \mathbf{M} = \frac{1}{V} \langle \sum_i \mathbf{s}_i \rangle. \quad (4)$$

The spontaneous magnetization $m_0(T)$ varies from $m_0 = 1$ for $T = 0$ to $m_0 \rightarrow 0$ for $T \rightarrow T_c$. Approaching the critical point, the magnetization $m_0(T)$ behaves as $m_0(T) \sim (T_c - T)^\beta$, where β is the magnetization critical exponent.

B. Off-equilibrium protocol

We are interested in the off-equilibrium dynamics arising in the presence of a time-dependent spatially-uniform magnetic field $\mathbf{H}(t)$ crossing the transition point $\mathbf{H} = 0$ at fixed temperature T . We assume that the direction of the magnetic field (vector \mathbf{e}) is fixed in the dynamics, while the component along \mathbf{e} varies as

$$h(t) = t/t_s, \quad (5)$$

where t_s is a time scale and we have chosen t so that $t = 0$ corresponds to $h = 0$. In the off-equilibrium protocol one starts from equilibrium configurations at an initial

value $h_i < 0$ at time $t_i < 0$. Then, the magnetic field is slowly changed up to a time $t_f > 0$, corresponding to a finite $h_f > 0$. This procedure is repeated several times, starting the dynamics from different equilibrium configurations at $h = h_i$. Observables are then averaged at fixed time t . As we shall see, in the limit $t_s \rightarrow \infty$ (very slow dynamics) the off-equilibrium scaling behavior around $t = 0$ is universal and does not depend on the initial value $h_i < 0$ of the magnetic field.

One can also consider a reversed process in which the magnetic field (5) varies from $h_i > 0$ to $h_f < 0$. Formally, it can be obtained by decreasing the *time* parameter from $t_i > 0$ to $t_f < 0$. This new process is of course identical to the original one, provided one changes the sign of t , h , and of the magnetization.

The off-equilibrium behavior depends on the particular time evolution of the system. There are several physically interesting cases, see, e.g., Refs. [37, 38]. In the following we present general scaling arguments that apply to any dynamics in which the slowest mode is associated with the magnetization. They will be verified numerically in Sec. IV for a purely relaxational dynamics.

C. Off-equilibrium scaling across the transitions

We present a scaling theory for the off-equilibrium dynamics of the magnetization across $h = 0$, in the quasi-adiabatic limit, i.e. for $t_s \rightarrow \infty$. In off-equilibrium processes driven by spatially uniform external fields, low-momentum modes, and in particular the magnetization, are expected to be the slowest modes of the system. The size dependence of the relevant scaling variables is parametrized by the effective RG scaling dimension y_h of the magnetic field and by the dynamic exponent z_m associated with the equilibrium dynamics of the magnetization. The determination of the appropriate values of y_h and z_m for the cases we consider, i.e., cubic and anisotropic cylinder-like systems, in the low-temperature phase and at T_c , is postponed to Sec. III.

The scaling theory is meant to describe the deviations of the statistical correlations from their equilibrium value, due to the fact that the system is not able to adapt itself to the changes of the magnetic field across $\mathbf{H} = 0$. Assuming the existence of a nontrivial scaling behavior for $h(t) \approx 0$ ($t \approx 0$, correspondingly), we expect the off-equilibrium behavior to be controlled by the two scaling variables

$$r_1 = h(t)L^{y_h} = (t/t_s)L^{y_h}, \quad r_2 = tL^{-z_m}. \quad (6)$$

In our context, it is convenient to use the equivalent scaling variables

$$u \equiv t_s^\kappa/L, \quad \kappa = \frac{1}{y_h + z_m}, \quad (7)$$

$$w \equiv t/t_s^{\kappa_t}, \quad \kappa_t = z_m\kappa, \quad (8)$$

which are combinations of r_1 and r_2 : $u = (r_2/r_1)^\kappa$ and $w = (r_1/r_2)^{\kappa_t}r_2$. Note that generally $\kappa_t < 1$.

We consider here a magnetic field that varies linearly with t , but one could analogously consider nonlinear behaviors such as $h(t) = \text{sgn}(t) |t/t_s|^n$ for $n > 0$. In this case the relevant scaling variables should be $r_1 = h(t)L^{y_h}$ and $r_2 = tL^{-z_m}$, which could be replaced by $u = t_s^\kappa/L$ and $w = t/t_s^{\kappa_t}$, with exponents $\kappa = n/(y_h + nz_m)$ and $\kappa_t = z_m\kappa$.

We now assume that the dynamics across the transition presents a scaling behavior when L , t_s , and t become large at fixed u and w . This implies the emergence of a length scale $\xi \sim t_s^\kappa$ and of a time scale $\tau \sim t_s^{\kappa_t}$ across the transition. The equilibrium static finite-size scaling (FSS) should be recovered in the limit $u, |w| \rightarrow \infty$ keeping $r_1 = w/u^{y_h}$ fixed. The off-equilibrium scaling behavior does not depend on the choice of the initial h_i and of the final h_f , because scaling occurs in a narrow range of values of $|h|$ that shrinks as $t_s \rightarrow \infty$. Indeed, the scaling behavior is observed in a time interval of size $\tau \sim t_s^{\kappa_t}$ around $t = 0$. Since $\kappa_t < 1$, we have $\tau/t_s \rightarrow 0$ in the large- t_s limit. Therefore, scaling occurs for smaller and smaller values of $|h|$. Note that this argument applies for any $T \leq T_c$.

Similar off-equilibrium scaling arguments have been reported in Refs. [8, 9, 39, 40] to describe other off-equilibrium systems driven by slowly-varying model parameters at phase transitions, such as the Kibble-Zurek mechanism. Actually, these off-equilibrium behaviors may be exploited to determine the equilibrium static and dynamic properties of critical systems, see, e.g., Ref. [41].

Let us now derive more quantitative predictions, considering first the dynamics at the critical point. The equilibrium magnetization (4) satisfies the scaling relation

$$m(L, h, T_c) \approx L^{-y_m} f_m(hL^{y_h}), \quad (9)$$

where

$$y_m = 3 - y_h = \frac{1 + \eta}{2}, \quad y_h = \frac{5 - \eta}{2}, \quad (10)$$

y_m is the RG dimension of the order parameter, and η is the critical exponent parametrizing the short-distance behavior of the two-point function. The behavior of $f_m(x)$ for large values of $|x|$ can be obtained by requiring Eq. (9) to be consistent with the finite- h infinite-volume behavior of the magnetization [42],

$$m(L = \infty, h, T_c) \approx \pm a|h|^{y_m/y_h} \quad \text{for } |h| \rightarrow 0, \quad (11)$$

where $a > 0$ and the \pm sign reflects the fact that m changes sign as $h \rightarrow -h$. Requiring the scaling formula (9) to reproduce Eq. (11) in the limit $L \rightarrow \infty$ for small nonvanishing values of $|h|$, we obtain for $|x| \rightarrow \infty$

$$f_m(x) \approx f_{\pm\infty}(x) \equiv \pm a|x|^{y_m/y_h}. \quad (12)$$

Indeed, if we substitute $f_m(x)$ with $f_{\pm\infty}(x)$ in Eq. (9) and use $x = hL^{y_h}$, we reobtain Eq. (11).

In order to describe the off-equilibrium regime around the transition point, we generalize Eq. (9) by writing

$$m(t, t_s, L; T = T_c) \approx L^{-y_m} F_m(u, w). \quad (13)$$

The *thermodynamic* infinite-volume limit (before taking the large t and t_s limits) can be formally obtained by performing the limit $u \rightarrow 0$ keeping w fixed, which leads to scaling expressions analogous to those discussed in Ref. [9]. Note that $F_m(u, w)$ is not expected to be symmetric for $w \rightarrow -w$ for finite values of u , because the off-equilibrium process is irreversible and therefore the time-reversal symmetry is violated (it is only recovered in the static FSS limit and for $|w| \rightarrow \infty$, see below).

The limit $|w| \rightarrow \infty$ of $F_m(u, w)$ at fixed u is expected to lead to the infinite-volume equilibrium behavior. Indeed, note first that, in a finite volume L , the slowest time scale — in our system the autocorrelation time τ_m associated with the magnetization — scales as L^{z_m} . A necessary condition to obtain equilibrium results is therefore that $t_s \gg \tau_m$, i.e., $t_s L^{-z_m} \rightarrow \infty$. At fixed u we have $t_s L^{-z_m} = u^{1/\kappa} L^{y_h}$ and hence the condition is satisfied for $L \rightarrow \infty$. Since we take the limit $w \rightarrow \infty$, we are considering the system at times t much larger than the time scale at which the off-equilibrium behavior occurs, so that the system is in equilibrium. Therefore, the scaling function $F_m(u, v)$ should match its equilibrium counterpart $f_m(r_1)$. Finally, since $r_1 = hL^{y_h} = wu^{-y_h}$, in the limit $w \rightarrow \infty$ at fixed u we have $r_1 \rightarrow \infty$, i.e., we are considering the behavior in the infinite-volume limit. Therefore, we expect

$$\begin{aligned} F_m(u, w) &\approx f_{+\infty}(wu^{-y_h}) = a(wu^{-y_h})^{y_m/y_h} \\ &= a u^{-y_m} w^{y_m/y_h}. \end{aligned} \quad (14)$$

In our discussion, we also need the corrections to the behavior (14). We now argue that the approach is exponentially fast. Note that, for $w \rightarrow \infty$, we are investigating the behavior of the system at finite (small) values of the magnetic field. For finite h and in infinite volume, we expect the deviations from equilibrium to decay exponentially in t with a typical time scale τ_h , i.e., as $\sim t^b e^{-t/\tau_h}$, where we have also included a power correction with exponent b . The time scale τ_h should be of order $\xi_h^{z_m}$ and the correlation length ξ_h should scale as h^{-1/y_h} . In the scaling limit at fixed w we have

$$\frac{t}{\tau_h} \sim t h^{z_m/y_h} = t^{z_m/y_h + 1} t_s^{-z_m/y_h} = t^\varepsilon t_s^{-\kappa \varepsilon} = w^\varepsilon, \quad (15)$$

where $\varepsilon = 1 + z_m/y_h = 1/(y_h \kappa) > 0$. Therefore, for large values of w , we expect

$$\frac{F_m(u, w)}{f_{+\infty}(wu^{-y_h})} - 1 \sim w^b \exp(-c w^\varepsilon), \quad (16)$$

where c should depend on u .

The same argument can be used to discuss the limit $w \rightarrow -\infty$. In this case, we start the dynamics at a very

large negative time t_i with $|t_i| \sim t_s$ in the magnetized phase with $h < 0$. Hence the previous arguments should apply also here, so that we predict, for $w \rightarrow -\infty$ at fixed u , the behavior

$$\frac{F_m(u, w)}{f_{-\infty}(wu^{-y_h})} - 1 \sim |w|^b \exp(-c |w|^\varepsilon), \quad (17)$$

Notice that the constant c and the exponent b entering here might well differ from those appearing in Eq. (16), while the exponent ε is expected to be the same.

The off-equilibrium scaling behavior (13) can be straightforwardly extended to other observables and correlation functions. Moreover, small deviations from T_c can be taken into account by adding a further dependence on the scaling variable $(T - T_c)L^{1/\nu}$.

The emergence of a universal static FSS behavior has been established also in the case of first-order transitions, see, e.g., Refs. [43–45]. In particular, Eq. (9) also holds at discontinuous transitions (a detailed discussion is presented in Sec. III A 2). It is therefore natural to conjecture that the off-equilibrium ansatz (13), with the appropriate exponents, applies also along the low-temperature first-order transition line. Since $m \rightarrow \pm m_0(T)$ for $h \rightarrow 0^\pm$, cf. Eq. (3), Eq. (12) formally requires $y_m = 0$ and $a = m_0(T)$. To avoid an additional nonuniversal normalization constant, it is convenient to introduce a *renormalized* magnetization defined as

$$m_r(t, t_s, L; T) \equiv \frac{m(t, t_s, L; T)}{m_0(T)}, \quad (18)$$

which satisfies $-1 \leq m_r \leq 1$. Therefore, in the low-temperature phase and for $t_s \rightarrow \infty$, we expect — we will verify it numerically below — the scaling behavior

$$m_r(t, t_s, L; T) \approx F_m(u, w), \quad (19)$$

where F_m is a universal scaling function, which takes values in the range $-1 \leq F_m \leq 1$ and satisfies all scaling expressions reported above. Using arguments analogous to those leading to Eqs. (16) and (17), we expect an exponential approach to the equilibrium behavior in the $w \rightarrow \pm\infty$ limits, i.e.

$$\begin{aligned} 1 - F_m(u, w) &\sim e^{-c_+ |w|^\varepsilon} \quad \text{for } w \rightarrow \infty, \\ -1 - F_m(u, w) &\sim -e^{-c_- |w|^\varepsilon} \quad \text{for } w \rightarrow -\infty, \end{aligned} \quad (20)$$

where again $\varepsilon = 1 + z_m/y_h$, and we have neglected possible powers of w in the prefactor.

We expect universality with respect to temperature changes in the low-temperature phase. This is supported by the fact that the effective scaling dimensions y_h and z_m do not depend on temperature for $T < T_c$ (but they differ from those at T_c), see sections III A 2 and III B 2. Universality also implies that the scaling function F_m does not depend on T , apart from a trivial renormalization of the scaling variables u and w .

One can also consider the time-reversed protocol, in which one starts at $h_i > 0$ and then decreases $h(t)$ to

$h_f < 0$, see Sec. II B. If $F_m^{(\text{inv})}(u, w)$ is the corresponding scaling function appearing in Eqs. (13) and (19), the symmetry of the model with respect to a reflection of the magnetic field implies

$$F_m^{(\text{inv})}(u, w) = -F_m(u, -w). \quad (21)$$

III. EQUILIBRIUM STATIC AND DYNAMIC BEHAVIOR

To verify the off-equilibrium scaling behaviors put forward in the previous section, we consider the Heisenberg $N = 3$ model. It presents a continuous transition at [46, 47] $T_c \approx 1.443$ (Ref. [46] obtained $\beta_c \equiv 1/T_c = 0.69300(1)$ by a FSS analysis of MC data), which separates the low-temperature ferromagnetic phase, in which the symmetry is spontaneously broken, from the high-temperature paramagnetic phase. In this section we review some general results for the static scaling behavior in a finite volume, both at $T = T_c$ and for $T < T_c$. We also discuss the dynamic equilibrium behavior for a relaxational dynamics, focusing, in particular, on the low-temperature phase.

A. Equilibrium finite-size scaling

1. Finite-size scaling at the critical point

At the critical point, the model shows a universal FSS depending on the static critical exponents. For the Heisenberg universality class they have been accurately estimated by various methods: see, e.g., Ref. [42] for a review of results. We mention the estimates [48, 49] $\nu = 0.7117(5)$ and $\eta = 0.0378(3)$ for the correlation-length and two-point function exponents, from which one can derive the magnetization exponent $\beta = \nu(1 + \eta)/2$.

At T_c , the magnetization behaves as reported in Eq. (9), with $y_m = 0.5189(2)$ and $y_h = 2.4811(2)$. The scaling function f_m is universal apart from trivial normalizations. However, it depends on the shape of the system and on the boundary conditions (but the critical exponents remain unchanged). Scaling corrections decay as $L^{-\omega}$, where the exponent ω is related to the RG dimension of the leading irrelevant operator [42]. Estimates of ω by various methods give $\omega \approx 0.78$ [50, 51].

2. Finite-size scaling at the first-order transition line

FSS in the low-temperature phase is more complex, because the relevant scaling variables depend both on the shape of the system and on the boundary conditions [44, 45, 52]. Fig. 1 shows some numerical results obtained by standard MC simulations at $T = 1$ and $\mathbf{H} = 0$, for cubic L^3 systems with PBC. Since $\mathbf{H} = 0$, we have $\mathbf{M} =$

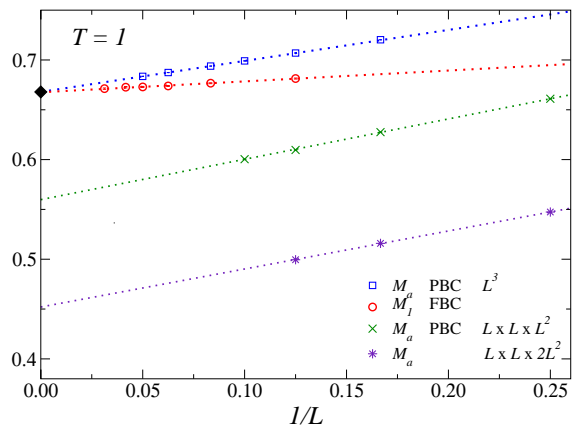


FIG. 1: (Color online) Finite-size magnetization in cubic L^3 systems and in anisotropic $L \times L \times L_{\parallel}$ systems for $T = 1$ and $\mathbf{H} = 0$. In the cubic case ($L_{\parallel} = L$) we report M_a defined in Eq. (22) for systems with PBC, and the component $M_1 = \mathbf{M} \cdot \mathbf{e}$ of the magnetization for systems with fixed boundary conditions (FBC): $\mathbf{s}_i = \mathbf{e} = (1, 0, 0)$ on the boundary. The finite-size results approach the same value $m_0(T)$ as $L \rightarrow \infty$, with L^{-1} corrections. The dotted lines correspond to linear fits to $M_{\infty} + b/L$, which lead to the large- L extrapolated estimates $M_{a,\infty} = 0.66804(4)$ and $M_{1,\infty} = 0.6676(6)$. In the anisotropic case we report M_a for $L_{\parallel} = L^2$ and $L_{\parallel} = 2L^2$. They also approach finite values $M_{a,\infty} < m_0(T)$, which depend on the ratio L^2/L_{\parallel} . Corrections are of order L^{-1} .

0 by symmetry. However, the related quantity

$$M_a = \frac{1}{V} \langle \left| \sum \mathbf{s}_i \right| \rangle \quad (22)$$

does not vanish, even in the large-volume limit. We compare the estimates of M_a with those of $M_1 = \mathbf{M} \cdot \mathbf{e}$ [here we take $\mathbf{e} = (1, 0, 0)$] computed in cubic systems with fixed boundary conditions (FBC) ($\mathbf{s}_i = \mathbf{e}$ on the boundary), whose large- L limit is expected to provide $m_0(T)$, cf. Eq. (3). As shown in Fig. 1, the extrapolated value of M_a is consistent with $m_0(T)$. For example, linear fits of M_a and M_1 at $T = 1$ to $M_{\infty} + b/L$ give $M_{a,\infty} = 0.66804(4)$ (PBC case) and $m_0 = M_{1,\infty} = 0.6676(6)$ (FBC case). These results confirm the arguments of Ref. [44]. They argued that in cubic systems the modulus of the magnetization is essentially constant and asymptotically equal to $m_0(T)$. On the other hand, its direction is randomly distributed in the sphere, to recover the $O(N)$ invariance. Spin waves give only rise to subleading contributions that decrease as $1/L$ [44]. We also note that $m_0(T)$ increases with decreasing T (we expect $m_0(T) \rightarrow 1$ for $T \rightarrow 0$). For example, at $T = 0.5$ we obtain $m_0(T) = 0.8600(3)$.

In the case of cubic systems with PBC the effective RG dimension y_h of the magnetic field is $y_h = d = 3$ [44]. Thus, we expect [44]

$$m(h, L; T) = m_0(T) f_m(hL^3), \quad f_m(0) = 0, \quad (23)$$

$$M_a(h, L; T) = m_0(T) f_a(hL^3), \quad f_a(0) = 1. \quad (24)$$

In particular, Ref. [44] obtains $f_m(hL^3) = I_{3/2}(y)/I_{1/2}(y)$ for $N = 3$, where $I_\nu(y)$ are the modified Bessel functions of the first kind and $y = m_0 h L^3$. Corrections, such as those due to spin-wave modes, are expected to decay as $1/L$ [44].

FSS is expected to substantially change in anisotropic geometries. If we consider systems of size $L \times L \times L_\parallel$ and $L_\parallel \gg L$, a finite longitudinal length scale [44] emerges along the longitudinal direction, which scales as $\xi_\parallel \sim L^2$. More precisely, for cylinder-like systems one can write the asymptotic scaling relation at $h = 0$ as

$$\xi_\parallel \approx L^2 f_\xi(L_\parallel/L^2), \quad (25)$$

where $f_\xi(x)$ is a scaling function, independent of T apart from trivial multiplicative normalizations. This implies that the effective scaling dimension of h in the FSS of $L \times L \times L_\parallel$ systems with $L_\parallel \sim L^2$ is $y_h = d + 1 = 4$. The FSS of the observables related to the magnetization reads [44]

$$m(h, L; T) \approx m_0(T) g_m(hL^4, L_\parallel/L^2), \quad (26)$$

$$M_a(h, L; T) \approx m_0(T) g_a(hL^4, L_\parallel/L^2), \quad (27)$$

where $g_{m,a}(x, y)$ are scaling functions. In particular, we expect $g_a(0, y \rightarrow 0) = 1$ and $g_a(0, y \rightarrow \infty) = 0$. These scaling behaviors are confirmed by the numerical results shown in Fig. 1 for M_a at $T = 1$ and $h = 0$, for $L_\parallel = L^2$ and $L_\parallel = 2L^2$. Note that the asymptotic value of M_a decreases with increasing L_\parallel/L^2 .

B. Equilibrium dynamic behavior under a relaxational dynamics

The off-equilibrium behavior depends on the dynamic universality class of the dynamics driving the system across the transition. It is generally characterized by the dynamic exponent z , which specifies the equilibrium large- L behavior of the autocorrelation time τ of the observables coupled to the slowest modes: $\tau \sim L^z$.

In the following we consider a purely relaxational dynamics, which can be realized by using the standard heat-bath [53] or Metropolis [54] algorithms in MC simulations.

1. Equilibrium dynamics at the critical point

At the critical point T_c , the dynamic exponent for the relaxational dynamics (model A of Ref. [37]) is very close to two. The dynamic exponent has been computed to three loops in perturbation theory [55] (see also Refs. [37, 38, 56]); its ϵ expansion can be expressed in terms of the exponent η as

$$z = 2 + c\eta, \quad c = 0.726 - 0.137\epsilon + O(\epsilon^2). \quad (28)$$

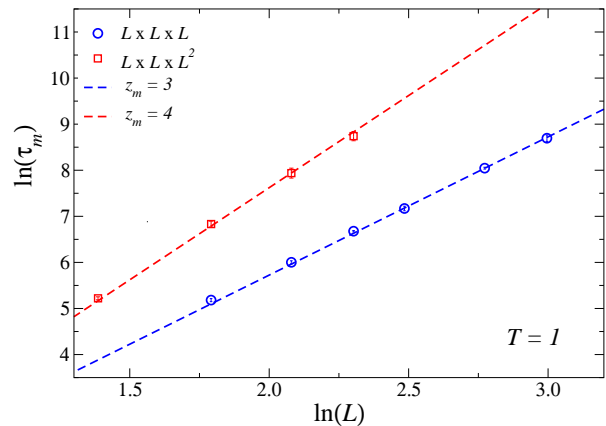


FIG. 2: (Color online) Autocorrelation time τ_m (in units of lattice sweeps) of the magnetization at $T = 1$ and $h = 0$ for the heat-bath dynamics [53]. We consider cubic $L \times L \times L$ systems and anisotropic $L \times L \times L^2$ systems, with PBC in all directions. The lines correspond to fits to $\tau_m = cL^{z_m}$, with $z_m = 3$ and $z_m = 4$ in the two cases, respectively.

Using the 3D estimate $\eta = 0.0378(3)$, this relation leads to the estimate $z = 2.02(1)$ for the 3D Heisenberg universality class, where the error takes somehow into account the uncertainty on the extrapolation to $\epsilon = 1$ of the three-loop ϵ -expansion result. In model-A systems the dynamic exponent z controls the equilibrium critical behavior of all observables associated with the critical modes, including the magnetization. Therefore, the exponent z_m entering the off-equilibrium scaling exponent κ defined in Eq. (7) should be identified with z : $z_m = z = 2.02(1)$.

Note that z not only depends on the static universality class, but also on the type of dynamics [37]. For instance, if the total magnetization is conserved in the dynamics, the critical dynamics for a Heisenberg ferromagnet is analogous to that of model J of Ref. [37], for which [37] $z = y_h = 2.4811(2)$.

2. Equilibrium dynamics at the first-order transition line

Let us now consider the dynamic behavior in the low-temperature case. For this purpose we perform MC simulations at $T = 1$ using the heat-bath dynamics [53]. Fig. 2 shows data [58] for the integrated autocorrelation time τ_m of the magnetization \mathbf{M} defined in Eq. (4). In the case of cubic L^3 systems, a fit of all data (L varies between 6 and 20) to $\tau_m = aL^{z_m}$ gives $z_m = 2.92(4)$. If we only consider data satisfying $L > 10$, we obtain $z_m = 3.00(15)$. Results are clearly consistent with $z_m = 3$: a fit of all data to $\tau_m = aL^3$ gives $\chi^2/\text{d.o.f.} \approx 1.0$ where d.o.f. is the number of degrees of freedom of the fit (the result is reported in Fig. 2).

In the case of cylinder-like systems ($L \times L \times L^2$), a fit of the magnetization integrated autocorrelation time ($4 \leq L \leq 10$) to $\tau_m = aL^{z_m}$ gives $z_m = 3.9(1)$. This result is clearly larger than that obtained in the cubic case and is

consistent with $z_m = 4$: a fit to $\tau_m = aL^4$ has $\chi^2/\text{d.o.f.} \approx 0.8$ (see Fig. 2). Also the autocorrelation time of M_a defined in Eq. (22) apparently increases as L^4 , at variance with the cubic case, in which the autocorrelation time of M_a is much smaller than that of m .

These numerical results suggest $z_m = 3$ for cubic L^3 systems and $z_m = 4$ for anisotropic cylinder-like systems, when PBC are considered. In the following we argue that they are exact values. We shall first present a heuristic argument, then a calculation using the Langevin dynamics for the ϕ^4 theory.

3. Theoretical predictions for the dynamic behavior of the magnetization

Let us first consider the case of fixed boundary conditions breaking the $O(N)$ symmetry, obtained by fixing the direction of the spins on the boundaries or introducing a boundary magnetic field. The average magnetization vector \mathbf{M} is essentially fixed: its modulus is approximately equal to $m_0(T)$ and its direction is fixed by the boundary conditions. In this case, the only relevant modes are spin waves (Goldstone modes). Since there are no critical fluctuations, the theory is expected to be Gaussian and therefore $z_m = 2$.

Let us now consider PBC or, more generally, any type of boundary conditions that do not break the $O(N)$ invariance. This case is different from that considered above. Indeed, while the modulus of the magnetization is again essentially fixed, there is no constraint on the direction of \mathbf{M} , whose rotation turns out to be the slowest dynamic mode of the system.

As we discussed in Sec. III A 2, in a finite volume the static behavior depends on the shape of the system. In the cubic case, the system is strongly correlated, so that all spins \mathbf{s}_i point in the same direction, with small random fluctuations. This implies that the modulus of the magnetization \mathbf{M} defined in Eq. (4) is essentially equal to $m_0(T)$ in the large- L limit. The direction of \mathbf{M} is however not fixed. Because of the relaxational dynamics, the vector $\mathbf{S} = \sum_i \mathbf{s}_i$ performs a random walk on the sphere of radius $|\mathbf{S}| \sim m_0(T)L^d$. Therefore, we expect that the number of random movements of the local site variables \mathbf{s}_i , which are required to significantly move the vector \mathbf{S} , scales as L^{2d} . This leads to the result $z_m = d$, taking into account that the time unit, i.e., a complete sweep of the lattice, consists of L^d local updatings.

A similar argument shows that, in anisotropic $L \times L \times L_{\parallel}$ systems with L_{\parallel}/L^2 fixed, the correct exponent is $z_m = 4$. In this case we should take into account the emergence of a longitudinal correlation length $\xi_{\parallel} \sim L^2$, which measures the correlations among the directions of the local magnetization (or its sum over L^2 slices) along the longitudinal direction (the one with length L_{\parallel}). As discussed in Ref. [44], the local magnetization is not uniformly directed along the longitudinal direction. However, the system can be partitioned in subsystems of size

$L \times L \times \xi_{\parallel}$, such that in each of them the spins \mathbf{s}_i are mostly oriented in the same direction, guaranteeing that the average magnetization $\boldsymbol{\mu}$ of the subsystem satisfies $|\boldsymbol{\mu}| \approx m_0(T)$. Assuming that the slowest modes are those related to the rotation of the average magnetization of each subsystem, the same argument used for cubic systems implies that $\tau_m \sim L^2 \xi_{\parallel} \sim L^4$, so that $z_m = 4$ for cylinder-like anisotropic systems.

We may obtain these results in a more quantitative way, considering the Langevin [57] dynamics in a $O(N)$ symmetric ϕ^4 theory. We assume for simplicity $N = 2$, considering a complex one-component field ϕ . However, the results hold for any $N \geq 2$. The Langevin equation controlling the dynamics is given by [37, 38]

$$\frac{\partial \phi(\mathbf{x}, t)}{\partial t} = -\frac{\Omega}{2} \left(-\nabla^2 \phi + r\phi + \frac{\lambda}{6} \phi |\phi|^2 \right) + \eta(\mathbf{x}, t), \quad (29)$$

where the random variables $\eta(\mathbf{x}, t)$ have a probability distribution proportional to

$$\exp \left[-\frac{1}{2\Omega} \int dt d\mathbf{x} |\eta(\mathbf{x}, t)|^2 \right]. \quad (30)$$

We will consider averages with respect to the random noise, which will be labelled with the angular brackets, i.e., with $\langle \cdot \rangle$.

In the low-temperature phase we have $r < 0$, the system is magnetized, and $|\phi(\mathbf{x}, t)|$ fluctuates around

$$a = \sqrt{-6r/\lambda}. \quad (31)$$

Therefore, we write

$$\phi(\mathbf{x}, t) = ae^{i\theta(\mathbf{x}, t)} [1 + \delta(\mathbf{x}, t)], \quad (32)$$

where $\delta(\mathbf{x}, t)$ is real and takes into account the fluctuations of $|\phi|$. Inserting this expression into Eq. (29) we obtain

$$i \frac{\partial \theta}{\partial t} (1 + \delta) + \frac{\partial \delta}{\partial t} = \frac{\Omega}{2} \left\{ e^{-i\theta} \nabla^2 [e^{i\theta} (1 + \delta)] - P(\delta) \right\} + e^{-i\theta} \eta/a, \quad (33)$$

where $P(\delta) = |r|\delta(1 + \delta)(2 + \delta)$. Separating real and imaginary parts we obtain

$$\begin{aligned} \frac{\partial \theta}{\partial t} (1 + \delta) &= \frac{\Omega}{2} [\nabla^2 \theta (1 + \delta) + 2\nabla \theta \cdot \nabla \delta] + \eta_{\theta}, \\ \frac{\partial \delta}{\partial t} &= -\frac{\Omega}{2} [(\nabla \theta)^2 (1 + \delta) - \nabla^2 \delta + P(\delta)] + \eta_{\delta}, \end{aligned} \quad (34)$$

where $\eta_{\theta}(\mathbf{x}, t)$ and $\eta_{\delta}(\mathbf{x}, t)$ have both probability distribution proportional to

$$\exp \left[-\frac{a^2}{2\Omega} \int dt d\mathbf{x} \eta_{\#}(\mathbf{x}, t)^2 \right]. \quad (35)$$

Now, we consider the evolution of θ and make the following assumptions.

- (i) We set $1 + \delta \approx 1$. This is quite natural as we expect δ to make small fluctuations around zero.
- (ii) We assume that δ and θ spatial fluctuations are uncorrelated, so that

$$\langle \nabla \theta \cdot \nabla \delta \rangle = 0. \quad (36)$$

These two assumptions are equivalent to those made in the heuristic argument. Essentially, we are decoupling the fluctuations of the modulus of the magnetization from its angular precession. If these two conditions hold, we obtain the linear equation

$$\frac{\partial \theta}{\partial t} = \frac{\Omega}{2} \nabla^2 \theta + \eta_\theta. \quad (37)$$

We consider a box of size $L_1 \times L_2 \times L_3$, $V = L_1 L_2 L_3$, and define

$$\theta(\mathbf{k}, t) = \int_V dx e^{i\mathbf{k} \cdot \mathbf{x}} \theta(\mathbf{x}, t), \quad (38)$$

$$\theta(\mathbf{x}, t) = \frac{1}{V} \sum_{\mathbf{k}} e^{-i\mathbf{k} \cdot \mathbf{x}} \theta(\mathbf{k}, t). \quad (39)$$

We obtain

$$\frac{\partial \theta(\mathbf{k}, t)}{\partial t} = -\frac{\Omega k^2}{2} \theta(\mathbf{k}, t) + \eta_\theta(\mathbf{k}, t), \quad (40)$$

where the probability distribution of $\eta_\theta(\mathbf{k}, t)$ is proportional to

$$\exp \left[-\frac{a^2}{2V\Omega} \int dt \sum_{\mathbf{k}} |\eta_\theta|^2 \right]. \quad (41)$$

The solution is

$$\theta(\mathbf{k}, t) = e^{-\Omega k^2 t/2} \int_0^t e^{\Omega k^2 s/2} \eta_\theta(\mathbf{k}, s) ds, \quad (42)$$

where we assume $\theta(\mathbf{k}, 0) = 0$. If we average over the random noise, we obtain

$$\langle \theta(\mathbf{k}, t)^* \theta(\mathbf{k}, s) \rangle = \frac{V}{a^2 k^2} \left(e^{-\Omega k^2 |t-s|/2} - e^{-\Omega k^2 (t+s)/2} \right). \quad (43)$$

If we now define the average angle

$$\Theta(t) = \frac{1}{V} \int d\mathbf{x} \theta(\mathbf{x}, t), \quad (44)$$

it follows

$$\langle \Theta(t) \rangle = 0 \quad \langle \Theta(t) \Theta(s) \rangle = \frac{\Omega}{2Va^2} (t+s - |t-s|), \quad (45)$$

or, equivalently,

$$\langle [\Theta(t) - \Theta(s)]^2 \rangle = \frac{\Omega}{a^2 V} |t-s|. \quad (46)$$

This shows that the average angle changes on time scales of order V . Let us now consider a ‘‘wall’’ quantity. If $\mathbf{x} = (x_1, x_2, x_3)$ we consider

$$\delta\theta_\perp(x_3, t) = \frac{1}{L_1 L_2} \sum_{x_1, x_2} [\theta(\mathbf{x}, t) - \Theta(t)] \quad (47)$$

and

$$G(t, s, r = x_3 - y_3) = \langle \delta\theta_\perp(x_3, t) \delta\theta_\perp(y_3, t) \rangle. \quad (48)$$

In the large-time limit, $t, s \rightarrow \infty$ at fixed $\tau = |t-s|$, i.e., at equilibrium, we can write it as

$$\begin{aligned} G(t, s, r) &= \frac{1}{a^2 V} \sum_{k_3 \neq 0} \frac{e^{-\Omega k_3^2 \tau/2}}{k_3^2} e^{ik_3 r} \\ &= \frac{L_3}{4\pi^2 a^2 L_1 L_2} \sum_{n \neq 0} \frac{e^{-n^2 \tilde{\tau}}}{n^2} e^{2\pi i n \tilde{r}}, \end{aligned} \quad (49)$$

where

$$\tilde{\tau} = 2\pi^2 \Omega \tau / L_3^2 \quad \tilde{r} = r / L_3. \quad (50)$$

There are, therefore, two different regimes. If $L_1 = L_2 = L_3 = L$ (cubic case) fluctuations are small (their variance decreases as $1/L$) and have a typical time scale of order L^2 . If instead, $L_1 = L_2 = L$ and $L_3 \propto L^2$, fluctuations are finite, but occur on significantly longer time and space scales $\tau \sim L^4$ and $r \sim L^2$. Note that, for τ large, the correlation function decreases exponentially, as $e^{-\tilde{\tau}}$.

At this point we can compute the autocorrelation function of the magnetization. Assuming that the size fluctuations are not relevant, we can write

$$\langle \mathbf{M}(s) \cdot \mathbf{M}(t) \rangle = \frac{a^2}{V^2} \int d\mathbf{x} d\mathbf{y} \langle e^{i[\theta(\mathbf{x}, s) - \theta(\mathbf{y}, t)]} \rangle. \quad (51)$$

In a cubic geometry, $\theta(\mathbf{x}, t) = \Theta(t) + O(1/\sqrt{L})$ so that

$$\begin{aligned} \langle \mathbf{M}(s) \cdot \mathbf{M}(t) \rangle &\approx a^2 \langle e^{i[\Theta(s) - \Theta(t)]} \rangle = \\ &a^2 e^{-\frac{1}{2} \langle [\Theta(s) - \Theta(t)]^2 \rangle} = a^2 \exp \left(-\frac{\Omega}{2a^2 V} |t-s| \right). \end{aligned} \quad (52)$$

The autocorrelation function has therefore a typical exponential shape with an autocorrelation time that scales as $V = L^3$. In the asymmetric case we should take into account the fluctuations along the longitudinal direction. Assuming a decoupling of the modes we obtain

$$\begin{aligned} \langle \mathbf{M}(s) \cdot \mathbf{M}(t) \rangle &\approx a^2 \exp \left(-\frac{\Omega}{2a^2 V} |t-s| \right) \times \\ &\frac{1}{L_3} \int_{-L_3/2}^{L_3/2} dr \exp[-G(t, s, r)/2]. \end{aligned} \quad (53)$$

In this case the behavior is more complex: in particular, we expect the amplitude of the time decay to be smaller than in the cubic case. However, the typical time dependence is still of order V , i.e., of order L^4 .

IV. NUMERICAL RESULTS

We now present numerical results obtained by MC simulations of the Heisenberg model, to check the off-equilibrium scaling ansatzes put forward in Sec. II C. We implement the protocol described in Sec. II B. We start from equilibrium configurations at an initial value $h_i < 0$ at $t_i < 0$. Then, the system evolves at fixed temperature by means of a heat-bath updating scheme [53]. The time unit is a sweep of the whole lattice, that is a heat-bath update at all sites. The magnetic field is changed according to Eq. (5) every sweep, incrementing t by one. The off-equilibrium relaxational dynamics ends at $t = t_f > 0$, corresponding to a finite $h_f = 1/32$. This procedure is repeated several times, averaging the observables at fixed time t . We will first consider the behavior at T_c , then at $T < T_c$.

A. Off-equilibrium scaling at T_c

We first verify the off-equilibrium scaling relation (13) for the magnetization at the critical point T_c . The relevant exponents for the Heisenberg $N = 3$ model are

$$y_m = 0.5189(2), \quad \kappa = 0.2222(5), \quad \kappa_t = 0.449(1), \quad (54)$$

obtained using the estimates $\eta = 0.0378(3)$ and $z = 2.02(1)$. In Fig. 3 we show the product $L^{y_m} m$ at fixed $u = t_s^\kappa / L$ versus $w = t/t_s^{\kappa_t}$, for $u \approx 0.735$ and $u = 1$. The results clearly approach u -dependent scaling curves with increasing L , nicely supporting the off-equilibrium scaling relation (13). Scaling corrections are expected to be controlled by the leading irrelevant operator, thus they should decay as $L^{-\omega}$ with $\omega \approx 0.78$. The data shown in the inset of Fig. 3 are consistent with this prediction.

The numerical results are also consistent with the asymptotic behaviors reported in Eqs. (16) and (17). To verify this explicitly we first determine the constant a , that appears in Eq. (14), by considering the large- $|w|$ behavior. For both values of u we have investigated, and both for $w \rightarrow +\infty$ and $w \rightarrow -\infty$, we obtain the same value $a \approx 0.745$, with a relative error that should be less than 1%. Then, we consider the quantity

$$Q_{\pm}(u, w) = 1 - \frac{L^{y_m} m(t, t_s, L)}{f_{\pm\infty}(wu^{-y_h})} \quad (55)$$

where the subscript \pm refers to positive and negative values of w . It is plotted in Fig. 4, showing that the data are consistent with the exponential decay predicted by Eqs. (16) and (17).

B. Off-equilibrium scaling for $T < T_c$

We now provide numerical evidence for the off-equilibrium scaling relation (19) along the first-order transition line $T < T_c$. The results for the equilibrium

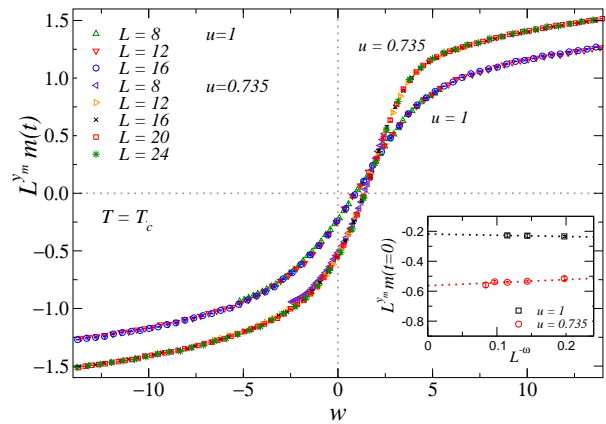


FIG. 3: (Color online) The rescaled magnetization $L^{y_m} m(t, t_s, L)$ during the off-equilibrium dynamics for cubic lattices at the critical point $T_c \approx 1.443$. We report data for $u = 0.735$ and $u = 1$, versus w , as defined in Eqs. (7) and (8). We use $\kappa = 0.2222$ and $\kappa_t = 0.449$, see Eq. (54). The inset shows $L^{y_m} m(t=0)$ vs $L^{-\omega}$ with $\omega = 0.78$, which is the expected behavior of the scaling corrections at T_c .

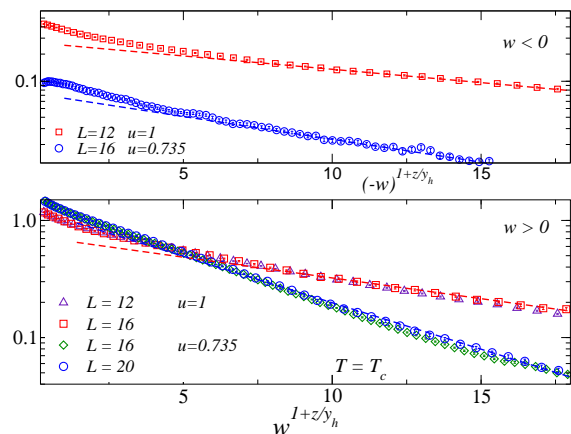


FIG. 4: (Color online) Semilogarithmic plot of Q_{\pm} , as defined in Eq. (55), for two values of u . We consider $w < 0$ (top) and $w > 0$ (bottom). Data are consistent with the exponential decay predicted by Eqs. (16) and (17). The straight lines are only meant to guide the eye.

static and dynamic FSS of Sec. III lead to the following values for the exponents κ and κ_t :

$$\kappa = 1/6, \quad \kappa_t = 1/2 \quad (\text{cubic}), \quad (56)$$

$$\kappa = 1/8, \quad \kappa_t = 1/2 \quad (\text{cylinder}), \quad (57)$$

where we used $y_h = 3$, $z_m = 3$ and $y_h = 4$, $z_m = 4$ for cubic and anisotropic cylinder-like systems, respectively.

One may qualitatively understand why z_m is the relevant dynamical exponent to be used to compute κ and κ_t in the low-temperature case. For $h < 0$ the total magnetization is aligned with \mathbf{H} . As h changes sign, \mathbf{M} should change its direction. As the system is magnetized, this is achieved by means of a rotation of \mathbf{M} , which takes a time of order V to be accomplished. During this time

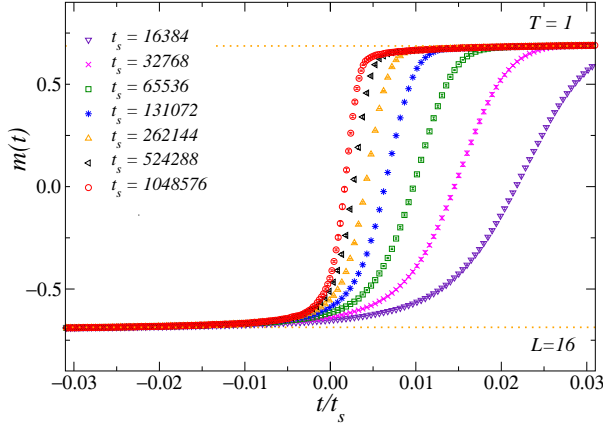


FIG. 5: (Color online) The magnetization as a function of t/t_s for cubic systems of size $L = 16$, for $T = 1$ and several values of t_s . The dotted lines correspond to $m = \pm m_0(T = 1)$ with $m_0(T = 1) \approx 0.668$, where $m_0(T)$ is the equilibrium spontaneous magnetization defined in Eq. (3).

interval the system is out of equilibrium and hence, the relevant time scale of the off-equilibrium dynamics scales as $V = L^{z_m}$, as we have used in the discussion.

To verify the theoretical predictions, we have carried out simulations at $T = 1$. Fig. 5 shows estimates of the magnetization as a function of t/t_s for cubic systems of linear size $L = 16$ and several values of t_s . For negative values of t , when $t/t_s \lesssim -0.01$ say, $m(t)$ is approximately equal to $-m_0(T)$, the spontaneous magnetization determined in equilibrium simulations at $h = 0$. The system is approximately in equilibrium, indicating that these values of t_s are sufficiently large compared with the relaxation time. As the transition point $h = 0$ is approached, the system is not able to adapt itself to the changes of the magnetic field. We note that the magnetization at $t = 0$ is always negative and it increases with increasing t_s . With increasing t_s , the behavior around $t = 0$ becomes sharper and sharper with respect to $h(t) = t/t_s$, to reconstruct the equilibrium discontinuity at $h = 0$. For $t_s \rightarrow \infty$ at fixed L we expect $m(t = 0) \rightarrow 0$, since the magnetization for $h = 0$ vanishes at equilibrium due to the $O(3)$ symmetry. We now show that this behavior around $t = 0$ can be described by the off-equilibrium scaling relation (19) for $t \approx 0$.

In order to verify that $u = t_s^\kappa/L$ with $\kappa = 1/6$ is the correct scaling variable for cubic systems, we note that Eq. (19) for $t = 0$ implies the relation

$$m_r(0, t_s, L) \approx g(u). \quad (58)$$

We expect $g(u)$ to be an increasing function of u , and in particular that $g(u \rightarrow 0) = -1$, and $g(u \rightarrow \infty) = 0$ due to the fact that at equilibrium $\langle \mathbf{M} \rangle = 0$ for $\mathbf{H} = 0$. Eq. (58) implies that data at $t = 0$ and fixed $u = t_s^\kappa/L$ must converge to nontrivial u -dependent values with increasing L . Fig. 6 shows data at some fixed values of u . They appear to converge to nontrivial values, supporting the predicted asymptotic behavior, with corrections which

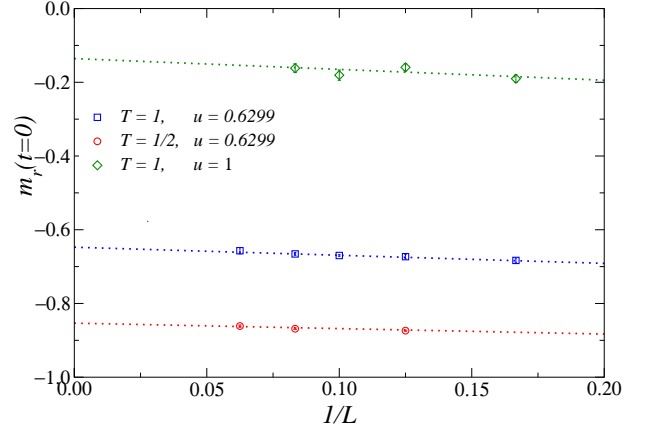


FIG. 6: (Color online) The renormalized magnetization m_r at $t = 0$ for cubic L^3 systems as a function of $1/L$. We report data for some values of $T < T_c$ and $u \equiv t_s^\kappa/L$ with $\kappa = 1/6$.

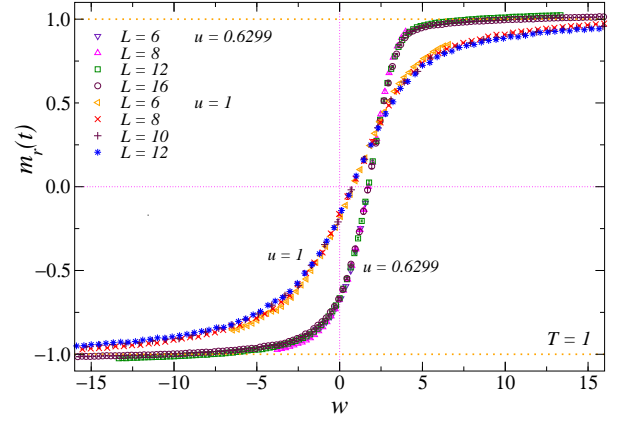


FIG. 7: (Color online) Scaling of the renormalized magnetization for cubic systems, as a function of $w \equiv t/t_s^\kappa$ with $\kappa_t = 1/2$. We report data for $T = 1$ and two values of the scaling variable $u = t_s^\kappa/L$ with $\kappa = 1/6$.

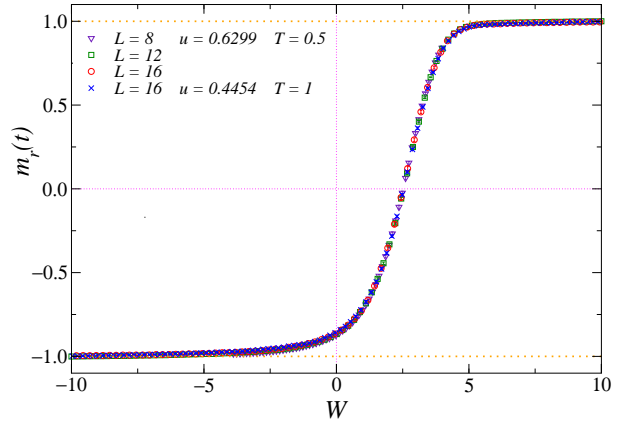


FIG. 8: (Color online) Scaling of the renormalized magnetization at $T = 0.5$ and $T = 1$ at the same value of $U = 0.6299$ (correspondingly $u = 0.4454$ for $T = 1$ and $u = 0.6299$ for $T = 0.5$) as a function of W ($w = W$ for $T = 0.5$ and $w = 0.9W$ for $T = 1$).

decay as L^{-1} , as expected. Note that the different values obtained at $T = 1$ and $T = 1/2$ for the same value of u do not contradict universality, because universality implies the same scaling function g apart from a normalization of the argument, see below.

The scaling with respect to $w = t/t_s^{\kappa_t}$ at fixed values of u is supported by the results reported in Figs. 7 and 8, where we show results for $T = 1$ and $T = 0.5$, respectively. In all cases the data at fixed values of u approach an asymptotic function of the scaling variable w , as predicted by the off-equilibrium scaling theory.

We expect that the scaling behavior (19) is universal with respect to changes of the temperature T as long as $T < T_c$. The scaling curves should be the same apart from trivial normalizations of the scaling variables u and w . To make universality more evident, we define new variables $U = c_u(T)u$ and $W = c_w(T)w$ so that

$$m_r(t, t_s, L, T) = \hat{F}_m(U, W), \quad (59)$$

where $\hat{F}_m(U, W)$ is universal and T independent. All temperature dependence is encoded in the two nonuniversal functions $c_u(T)$ and $c_w(T)$. They are uniquely specified only if two normalization conditions are given. For example, one can fix the scaling function for two particular values of U and W , or specify $c_u(T)$ and $c_w(T)$ at a given temperature. In the following we require $c_u(T) = c_w(T) = 1$ for $T = 0.5$. To perform a universality check using data at $T = 0.5$ and $T = 1$, we should determine $c_u(T)$ and $c_w(T)$ for $T = 1$. To determine the former quantity, we consider data at $t = 0$ (correspondingly $w = 0$) and note that the data for $T = 1$ at $u = 0.4454$ and $T = 0.5$ at $u = 0.6299$ both give $m_r(t = 0) \approx -0.86$ for $L \rightarrow \infty$. This implies $c_u(T = 1) \approx 0.6299/0.4454 = 1.414$. To determine $c_w(T = 1)$ we consider the results for the same value of U (we take $U = 0.6299$) and require the data to collapse once plotted as a function of W . We obtain $c_w(T = 1) \approx 1.1$. The results for $T = 1$ and $T = 0.5$ at the same value of U are shown in Fig. 8 as a function of W : all data fall onto the same scaling curve, nicely confirming universality.

Analogous results are obtained in the case of cylinder-like systems, when using the corresponding scaling exponents given in Eq. (57). In Fig. 9 we show the renormalized magnetization for a system of size $L \times L \times L^2$. Results at fixed $u = t_s^\kappa/L$ with $\kappa = 1/8$ are plotted versus $w = t/t_s^{\kappa_t}$ with $\kappa_t = 1/2$. The data appear to collapse toward scaling curves, confirming the correctness of the scaling Ansatz (19) with the exponents (57).

V. HYSTERESIS PHENOMENA

As shown in the previous sections, the system is unable to reach equilibrium when it goes through the transition point at $h = 0$. To quantify the departure from equilibrium we can consider protocols in which the magnetic

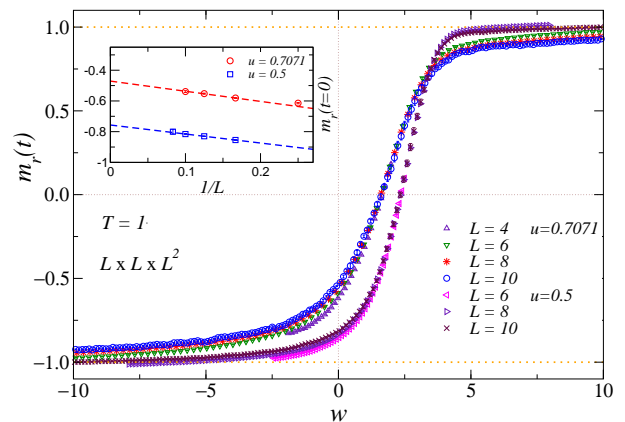


FIG. 9: (Color online) Estimates of the renormalized magnetization for anisotropic lattices of size $L^2 \times L_{\parallel}$ with $L_{\parallel} = L^2$. We report data for $T = 1$ and $u = t_s^\kappa/L = 0.7071, 0.5$ (with $\kappa = 1/8$), versus the scaling variable $w \equiv t/t_s^{\kappa_t}$ (with $\kappa_t = 1/2$). The inset shows $m_r(t = 0)$ vs $1/L$, which is the expected behavior of the scaling corrections.

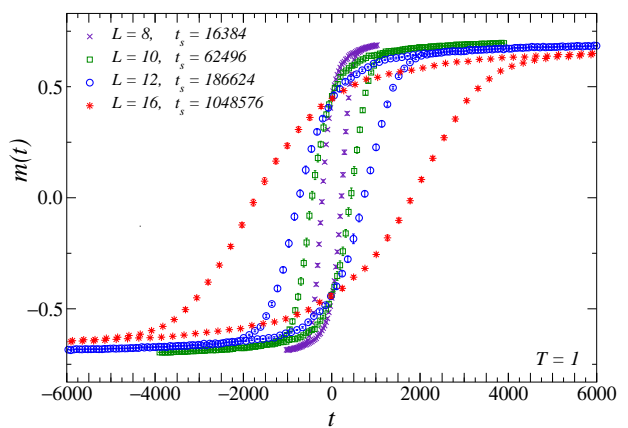


FIG. 10: (Color online) Hysteresis loops of the magnetization for cubic systems at $T = 1$ versus the time parameter t , for several values of L and t_s . We consider a round-trip protocol: first t increases from $t_i < 0$ to $t_f > 0$ (correspondingly, we have $h_i = -1/16$ and $h_f = 1/16$), then it decreases back to $t_i < 0$.

field is slowly increased from $h_i < 0$ to $h_f > 0$ and then it is decreased back again to $h_i < 0$. In this case the magnetization shows a hysteresis loop, whose area

$$A_h = - \oint dt m(t) \quad (60)$$

provides a quantitative indication of how far the system is out of equilibrium.

In Fig. 10 we show some examples of hysteresis loops for the magnetization for cubic systems at $T = 1$. Here we start at $t_i < 0$ ($h_i = -1/16$), increase t until $h = h_f = 1/16$, then decrease t back to t_i . The arguments presented in the previous sections imply that also the hysteresis loops have a scaling behavior. Scaling plots are shown in Fig. 11 for $T = 1$ and in Fig. 12 at the critical

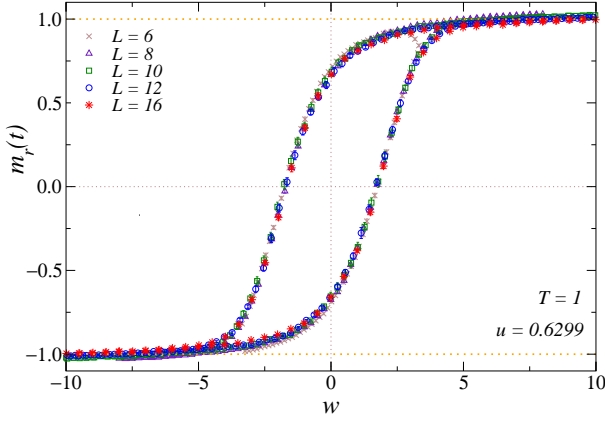


FIG. 11: (Color online) Hysteresis loop of the renormalized magnetization m_r defined in Eq. (18) for cubic L^3 systems at $T = 1$. We report data at fixed $u \approx 0.6299$ versus w . We consider a round-trip protocol: first t increases from $t_i < 0$ to $t_f > 0$ (correspondingly, we have $h_i = -1/16$ and $h_f = 1/16$), then it decreases back to $t_i < 0$.

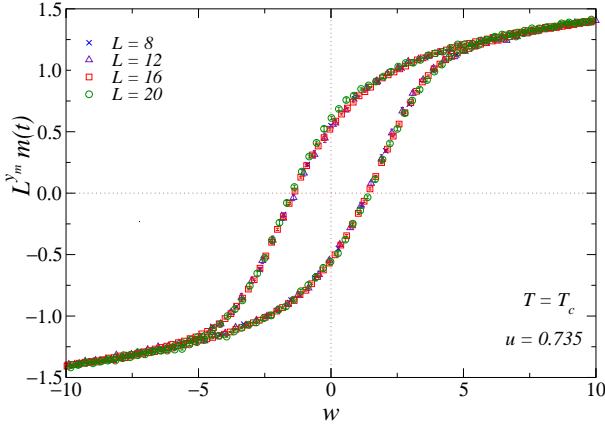


FIG. 12: (Color online) Plot of $L^{y_m} m(t)$ for cubic L^3 systems at the critical point T_c . We report data at fixed $u \approx 0.735$ versus w . We consider a round-trip protocol: first t increases from $t_i < 0$ to $t_f > 0$ (correspondingly, we have $h_i = -1/16$ and $h_f = 1/16$), then it decreases back to $t_i < 0$.

point. It should be noted that, while the magnetization shows a clear hysteresis cycle, there is no evidence of such a phenomenon for the energy. In Fig. 13 we show the time dependence of the energy density at $T = 1$ obtained using the same round-trip protocols considered in Fig. 10. Within the precision of our data, there is no evidence of hysteresis.

In practice, since time is discretized in our MC simulations we measure $m(t)$ at discrete values t_j of t , the area enclosed by the hysteresis loop of the magnetization can be computed using the area estimator

$$B_h \equiv \Delta \sum_j [m(t_j, t_s, L)_{h_f \rightarrow h_i} - m(t_j, t_s, L)_{h_i \rightarrow h_f}], \quad (61)$$

where $\Delta \equiv t_{j+1} - t_j$ is the time interval between two measurements.

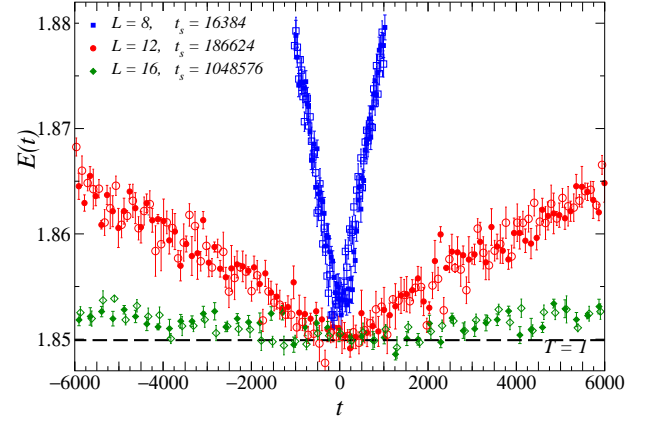


FIG. 13: (Color online) Time dependence of the energy density at $T = 1$ along the same round-trip protocols considered in Fig. 10: first t increases from $t_i < 0$ to $t_f > 0$ (full symbols), correspondingly, we have $h_i = -1/16$ and $h_f = 1/16$, then it decreases back to $t_i < 0$ (open symbols). There is no evidence of hysteresis within the precision of our data. The dashed line corresponds to the equilibrium value for $h = 0$.

Using the scaling relations (13) and (19) for the magnetization, we can express the area in terms of the scaling functions $F_m(u, v)$ and $F_m^{(\text{inv})}(u, w)$ of the reverse process in which time decreases. At the critical point T_c , we obtain

$$\begin{aligned} A_h &\approx L^{-y_m} t_s^{\kappa_t} \int_{-\infty}^{\infty} dw [F_m^{(\text{inv})}(u, w) - F_m(u, w)] \quad (62) \\ &= -L^{y_m} t_s^{\kappa_t} \int_{-\infty}^{\infty} dw [F_m(u, w) + F_m(u, -w)], \end{aligned}$$

where relation (21) has been used to arrive at the second line. Using the asymptotic relation (16), it is immediate to show that the integral (62) is finite. We can therefore define a universal scaling function $\mathcal{A}(u)$ associated with the area of the hysteresis loop:

$$\begin{aligned} A_h &\approx L^{-y_m} t_s^{\kappa_t} \mathcal{A}(u), \quad (63) \\ \mathcal{A}(u) &= - \int_{-\infty}^{\infty} dw [F_m(u, w) + F_m(u, -w)]. \end{aligned}$$

We expect $\mathcal{A}(u)$ to be a decreasing function of u , and in particular $\mathcal{A}(u) \rightarrow 0$ in the static limit $u \rightarrow \infty$. The scaling relation (63) can also be written as

$$A_h \approx L^{z_m - y_m} u^{z_m} \mathcal{A}(u), \quad (64)$$

where $z_m - y_m = 3/2 + (c - 1/2)\eta$, see Eqs. (10) and (28). For the Heisenberg model we have $z_m - y_m \approx 1.50$, so that A_h increases with L at fixed u .

Proceeding analogously, in the low-temperature phase $T < T_c$ we obtain

$$\begin{aligned} A_h &\approx m_0(T) t_s^{\kappa_t} \mathcal{A}(u), \quad (65) \\ \mathcal{A}(u) &= - \int_{-\infty}^{\infty} dw [F_m(u, w) + F_m(u, -w)], \end{aligned}$$

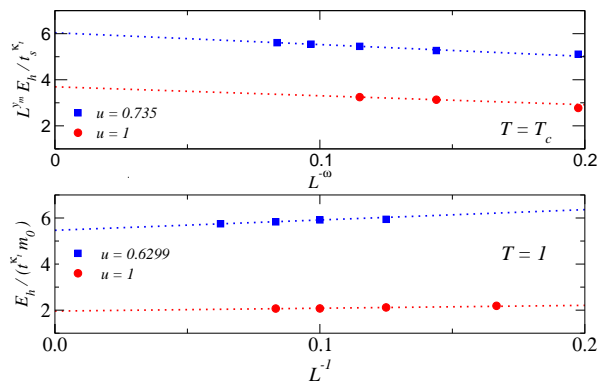


FIG. 14: (Color online) Hysteresis loop area at $T = T_c$ (top) and at $T = 1$ (bottom). We report $t_s^{-\kappa_t} L^{z_m} E_h$ versus $L^{-\omega}$ in the case of $T = T_c$ (here we use $\kappa = 0.2222$ and $\kappa_t = 0.449$), and $t_s^{-\kappa_t} m_0(T)^{-1} E_h$ versus L^{-1} in the $T = 1$ case (here we use $\kappa = 1/6$ and $\kappa_t = 1/2$). The dotted lines correspond to linear fits of the data for the largest available sizes.

where F_m is the scaling function entering Eq. (19). Eq. (65) can be also written as $A_h \approx L^{z_m} u^{z_m} \mathcal{A}(u)$. We stress that the scaling behavior of the hysteresis loop area does not depend on the chosen values $h_i < 0$ and $h_f > 0$, as already discussed in Sec. II C.

By exploiting the parity symmetry leading to the relation (21), the hysteresis loop area can be estimated by only using data of the one-way protocol from $h_i < 0$ to $h_f > 0$, introduced in Sec. II B. This allows us to define an improved estimator E_h

$$\begin{aligned} E_h(t_s, L; T) &\equiv \Delta \sum_j [m(-t_j, t_s, L) - m(t_j, t_s, L)] \\ &= -2\Delta \sum_j m(t_j, t_s, L), \end{aligned} \quad (66)$$

which has a smaller statistical errors than B_h defined in Eq. (61). In Fig. 14 we report E_h for $T = 1$ and $T = T_c$ at some fixed values of u . In order to check the scaling behaviors (62) and (65), we plot $t_s^{-\kappa_t} L^{z_m} E_h$ versus $L^{-\omega}$ in the case of $T = T_c$, and $t_s^{-\kappa_t} m_0(T)^{-1} E_h$ versus L^{-1} in the $T = 1$ case. The results linearly extrapolate to constant values, supporting the predicted off-equilibrium scaling behaviors (62) and (65). The estimator B_h gives consistent results.

VI. CONCLUSIONS

We consider systems with a continuous global symmetry in the presence of slowly-varying time-dependent external fields. More specifically, we focus on the 3D $O(N)$ vector model with $N \geq 2$ coupled to a time-dependent spatially uniform magnetic field $\mathbf{H}(t)$. We assume $\mathbf{H}(t) = h(t) \mathbf{e}$, where $h(t) = t/t_s$, t_s is a time scale, and \mathbf{e} is a constant unit N -component vector. In practice, the dynamics starts from equilibrium configurations at an initial value $h_i < 0$ at time $t_i < 0$. Then,

the magnetic field is slowly varied, up to a time $t_f > 0$ corresponding to a finite $h_f > 0$. For $t \approx 0$, i.e. when the magnetic field h changes sign, the system is no longer in equilibrium, for any temperature $T \leq T_c$, where T_c is the critical temperature.

In the adiabatic limit $t_s \rightarrow \infty$, the off-equilibrium behavior turns out to be universal. By using scaling arguments, we derive a general scaling theory for the dynamics across the transition line $h = 0$. In particular, the magnetization shows universal scaling behaviors in terms of appropriate combinations of the time t , the time scale t_s , and the finite size L , in the large- L , t_s, t limit. Heuristic scaling arguments allow us to identify the relevant scaling variables, which can be expressed as t_s^κ/L and $t/t_s^{\kappa_t}$, where κ and κ_t are appropriate exponents. In other words, as the system slowly moves through the transition line $h = 0$, the dynamics is controlled by a new length scale $\xi \sim t_s^\kappa$ and by a time scale $\tau \sim t_s^{\kappa_t}$. We stress that this is not specific of the continuous transition at T_c . The same scaling theory, but with different exponents, applies in the low-temperature phase $T < T_c$, where the system undergoes a first-order transition at $h = 0$.

The exponents κ and κ_t depend on the equilibrium static and dynamic exponents which describe the equilibrium static and dynamic FSS behavior of the system at fixed temperature. Static FSS is recovered as a particular limit of the off-equilibrium scaling ansatzes. For $T < T_c$ the exponents do not vary with the temperature, but depend on the boundary conditions and on the geometry of system. In particular, the exponents for cubic $L \times L \times L$ systems are different from those appropriate for anisotropic cylinder-like systems of size $L \times L \times L_\parallel$ with $L_\parallel \gg L$. Such a phenomenon does not occur at T_c : here the exponents do not depend on the shape and on the boundary conditions (however, scaling functions do depend on these features).

We present MC numerical results for the 3D Heisenberg ($N = 3$) model. We use a heat-bath updating scheme, which is a particular example of a purely relaxational dynamics (sometimes named as model-A dynamics [37]). The results provide a robust numerical evidence of the off-equilibrium scaling theory we have put forward, both at the critical point T_c and for $T < T_c$. Note that the general theory should hold for any $N \geq 2$ in three dimensions, and it should also apply to other types of dynamics, provided one uses the appropriate value for the dynamic exponent.

We also discuss the hysteresis phenomena which generally arise in off-equilibrium conditions when round-trip protocols are used. We consider again the time-dependent external field $h(t) = t/t_s$, but now we vary t first from $t_i < 0$ to $t_f > 0$, and then back from t_f to t_i . The area enclosed by the hysteresis curve of the magnetization may be considered as a measure of how far the system is from equilibrium. The hysteresis loop area satisfies a nontrivial scaling behavior at and below T_c , as a function of the scaling variable t_s^κ/L .

In the case of discrete symmetries, such as the Ising ($N = 1$) model or the Potts models, the off-equilibrium behavior in the low-temperature phase may be even more complex than the one discussed here. As already suggested by studies of classical and quantum systems with discrete symmetry [39, 40, 43, 45], the off-equilibrium behavior is expected to be particularly sensitive to the boundary conditions. In particular, drastically different behaviors may be observed, depending on the presence/absence of an interface in the system.

As mentioned in the introduction, off-equilibrium phenomena arising from slow changes of model parameters through phase transitions are of great theoretical and

experimental interest. They have been investigated in several experiments on different physical systems, see, e.g., Refs. [7, 14–36]. Most investigations have been performed at continuous classical and quantum transitions. We have shown here that analogous scaling behaviors can be observed at first-order transitions, with some peculiar features. We believe that theoretical and experimental investigations of these issues may lead to a substantial progress in the understanding of dynamic phenomena at first-order classical and quantum transitions, which are observed in many different physical systems, from magnetic to cold-atom systems, both at finite temperature and in the zero-temperature limit.

-
- [1] K. Binder, Theory of first-order phase transitions, Rep. Prog. Phys. **50**, 783 (1987).
- [2] T. W. B. Kibble, Topology of cosmic domains and strings, J. Phys. A **9**, 1387 (1976).
- [3] W. H. Zurek, Cosmological experiments in superfluid helium?, Nature **317**, 505 (1985).
- [4] P. Calabrese and A. Gambassi, Ageing Properties of Critical Systems, J. Phys. A **38**, R133 (2005).
- [5] A. Polkovnikov, K. Sengupta, A. Silva, and M. Vengalattore, Colloquium: Nonequilibrium dynamics of closed interacting quantum systems, Rev. Mod. Phys. **83**, 863 (2011).
- [6] G. Biroli, Slow Relaxations and Non-Equilibrium Dynamics in Classical and Quantum Systems, arXiv:1507.05858.
- [7] M. J. Davis, T. M. Wright, T. Gasenzer, S. A. Gardiner, and N. P. Proukakis, Formation of Bose-Einstein condensates, arXiv:1601.06197.
- [8] S. Gong, F. Zhong, X. Huang, and S. Fan, Finite-time scaling via linear driving, New J. Phys. **12**, 043036 (2010).
- [9] A. Chandran, A. Erez, S. S. Gubser, and S. L. Sondhi, Kibble-Zurek problem: Universality and the scaling limit, Phys. Rev. B **86**, 064304 (2012).
- [10] W.H. Zurek, U. Dorner, and P. Zoller, Dynamics of a Quantum Phase Transition, Phys. Rev. Lett. **95**, 105701 (2005); J. Dziarmaga, Dynamics of a Quantum Phase Transition: Exact Solution of the Quantum Ising Model, Phys. Rev. Lett. **95**, 245701 (2005); A. Polkovnikov, Universal adiabatic dynamics in the vicinity of a quantum critical point, Phys. Rev. B **72**, 161201(R) (2005).
- [11] A. Polkovnikov and V. Gritsev, Breakdown of the adiabatic limit in low-dimensional gapless systems, Nature Phys. **4**, 477 (2008).
- [12] A. Chandran, A. Nanduri, S. S. Gubser, and S. L. Sondhi, On equilibration and coarsening in the quantum $O(N)$ model at infinite N , Phys. Rev. B **88**, 024306 (2013).
- [13] A. Francuz, J. Dziarmaga, B. Gardas, W. H. Zurek, Space-time renormalization in phase transition dynamics, arXiv:1510.06132.
- [14] I. Chuang, R. Durrer, N. Turok, and B. Yurke, Cosmology in the Laboratory: Defect Dynamics in Liquid Crystals, Science **251**, 1336 (1991).
- [15] M. J. Bowick, L. Chandar, E. A. Schiff, and A. M. Srivastava, The Cosmological Kibble Mechanism in the Laboratory: String Formation in Liquid Crystals, Science **263**, 943 (1994).
- [16] C. Bäuerle, Yu M. Bunkov, S. N. Fisher, H. Godfrin, and G. R. Pickett, Laboratory simulation of cosmic string formation in the early Universe using superfluid ^3He , Nature **382**, 332 (1996).
- [17] V. M. H. Ruutu, V. B. Eltsov, A. J. Gill, T. W. B. Kibble, M. Krusius, Y. G. Makhlin, B. Placais, G. E. Volovik, and W. Xu, Vortex formation in neutron-irradiated superfluid ^3He as an analogue of cosmological defect formation, Nature **382**, 334 (1996).
- [18] R. Carmi, E. Polturak, and G. Koren, Observation of Spontaneous Flux Generation in a Multi-Josephson-Junction Loop, Phys. Rev. Lett. **84**, 4966 (2000).
- [19] S. Casado, W. González-Viñas, H. Mancini, and S. Boccaletti, Topological defects after a quench in a Benard-Marangoni convection system, Phys. Rev. E **63**, 057301 (2001).
- [20] R. Monaco, J. Mygind, and R. J. Rivers, Observation of Spontaneous Flux Generation in a Multi-Josephson-Junction Loop, Phys. Rev. Lett. **89**, 080603 (2002).
- [21] A. Maniv, E. Polturak, and G. Koren, Observation of Magnetic Flux Generated Spontaneously During a Rapid Quench of Superconducting Films, Phys. Rev. Lett. **91**, 197001 (2003).
- [22] S. Casado, W. González-Viñas, and H. Mancini, Observation of Magnetic Flux Generated Spontaneously During a Rapid Quench of Superconducting Films, Phys. Rev. E **74**, 047101 (2006).
- [23] R. Monaco, J. Mygind, M. Aaroe, R. J. Rivers, and V.P. Koshelets, Zurek-Kibble Mechanism for the Spontaneous Vortex Formation in NbAl/Alox/Nb Josephson Tunnel Junctions: New Theory and Experiment, Phys. Rev. Lett. **96**, 180604 (2006).
- [24] L.E. Sadler, J.M.Higbie, S.R. Leslie, M. Vengalattore, and D.M. Stamper-Kurn, Spontaneous symmetry breaking in a quenched ferromagnetic spinor Bose-Einstein condensate, Nature **443**, 312 (2006).
- [25] C.N. Weiler, T. W. Neely, D. R. Scherer, A. S. Bradley, M. J. Davis and B. P. Anderson, Spontaneous vortices in the formation of Bose-Einstein condensates, Nature **455**, 948 (2008).
- [26] D. Golubchik, E. Polturak, and G. Koren, Evidence for Long-Range Correlations within Arrays of Spontaneously Created Magnetic Vortices in a Nb Thin-Film Supercon-

- ductor, Phys. Rev. Lett. **104**, 247002 (2010).
- [27] D. Chen, M. White, C. Borries, and B. DeMarco, Quantum Quench of an Atomic Mott Insulator, Phys. Rev. Lett. **106**, 235304 (2011).
- [28] S. C. Chae, N. Lee, Y. Horibe, M. Tanimura, S. Mori, B. Gao, S. Carr, and S.-W. Cheong Direct Observation of the Proliferation of Ferroelectric Loop Domains and Vortex-Antivortex Pairs, Phys. Rev. Lett. **108**, 167603 (2012).
- [29] M.A. Miranda, J. Burguete, H. Mancini, and W. González-Viñas, Phys. Rev. E **87**, 032902 (2013).
- [30] S. Ejtemaei and P. C. Haljan, Spontaneous nucleation and dynamics of kink defects in zigzag arrays of trapped ions, Phys. Rev. A **87**, 051401(R) (2013).
- [31] S. Ulm, S. J. Ronagel, G. Jacob, C. Degünther, S. T. Dawkins, U. G. Poschinger, R. Nigmatullin, A. Retzker, M. B. Plenio, F. Schmidt-Kaler, and K. Singer, Observation of the Kibble-Zurek scaling law for defect formation in ion crystals, Nat. Commun. **4**, 2290 (2013).
- [32] K. Pyka, J. Keller, H. L. Partner, R. Nigmatullin, T. Burgermeister, D. M. Meier, K. Kuhlmann, A. Retzker, M. B. Plenio, W. H. Zurek, A. del Campo, and T. E. Mehlstäubler, Topological defect formation and spontaneous symmetry breaking in ion Coulomb crystals, Nat. Commun. **4**, 2291 (2013).
- [33] G. Lamporesi, S. Donadello, S. Serafini, F. Dalfovo, and G. Ferrari, Spontaneous creation of Kibble-Zurek solitons in a Bose-Einstein condensate, Nat. Phys. **9**, 656 (2013).
- [34] L. Corman, L. Chomaz, T. Bienaimé, R. Desbuquois, C. Weitenberg, S. Nascimbene, J. Dalibard, and J. Beugnon, Quench-Induced Supercurrents in an Annular Bose Gas, Phys. Rev. Lett. **113**, 135302 (2014).
- [35] N. Navon, A. L. Gaunt, R. P. Smith, and Z. Hadzibabic, Critical Dynamics of Spontaneous Symmetry Breaking in a Homogeneous Bose gas, Science **347**, 167 (2015).
- [36] S. Braun, M. Friesdorf, S.S. Hodgman, M. Schreiber, J.P. Ronzheimer, A. Riera, M. del Rey, I. Bloch, J. Eisert, and U. Schneider, Emergence of coherence and the dynamics of quantum phase transitions, PNAS **112**, 3641 (2015).
- [37] P. C. Hohenberg and B. I. Halperin, Theory of dynamic critical phenomena, Rev. Mod. Phys. **49**, 435 (1977).
- [38] R. Folk and G. Moser, Critical dynamics: a field-theoretical approach, J. Phys. A **39**, R207 (2006).
- [39] M. Campostrini, A. Pelissetto, and E. Vicari, Quantum transitions driven by one bond defect in quantum Ising rings, Phys. Rev. E **91**, 042123 (2015); Quantum Ising chains with boundary fields, J. Stat. Mech. (2015) P11015.
- [40] H. Panagopoulos and E. Vicari, Off-equilibrium scaling across a first-order transition, Phys. Rev. E **92**, 062107 (2015).
- [41] C.-W. Liu, A. Polkovnikov, A. W. Sandvik, and A. P. Young, Universal dynamic scaling in three-dimensional Ising spin glasses, Phys. Rev. E **92**, 022128 (2015).
- [42] A. Pelissetto and E. Vicari, Critical Phenomena and Renormalization Group Theory, Phys. Rep. **368**, 549 (2002).
- [43] V. Privman and M. E. Fisher, Finite-size effects at first-order transitions, J. Stat. Phys. **33**, 385 (1983).
- [44] M. E. Fisher and V. Privman, First-order transitions breaking $O(n)$ symmetry: Finite-size scaling, Phys. Rev. B **32**, 447 (1985).
- [45] M. Campostrini, J. Nespolo, A. Pelissetto, and E. Vicari, Finite-size scaling at first-order quantum transitions, Phys. Rev. Lett. **113**, 070402 (2014); Finite-size scaling at first-order quantum transitions of quantum Potts chains, Phys. Rev. E **91**, 052103 (2015).
- [46] H. G. Ballesteros, L. A. Fernandez, V. Martin-Mayor, and A. Muñoz Sudupe, Finite size effects on measures of critical exponents in $d = 3$ $O(N)$ models, Phys. Lett. B **387**, 125 (1996).
- [47] P. Butera and M. Comi, N -vector spin models on the simple-cubic and the body-centered-cubic lattices: A study of the critical behavior of the susceptibility and of the correlation length by high-temperature series extended to order β^{21} , Phys. Rev. B **56**, 8212 (1997).
- [48] M. Hasenbusch and E. Vicari, Anisotropic perturbations in 3D $O(N)$ vector models, Phys. Rev. B **84**, 125136 (2011).
- [49] M. Campostrini, M. Hasenbusch, A. Pelissetto, P. Rossi, and E. Vicari, Critical exponents and equation of state of the three-dimensional Heisenberg universality class, Phys. Rev. B **65**, 144520 (2002).
- [50] R. Guida and J. Zinn-Justin, Critical exponents of the N -vector model, J. Phys. A **31**, 8103 (1998).
- [51] M. Hasenbusch, Eliminating leading corrections to scaling in the three-dimensional $O(N)$ -symmetric ϕ^4 model: $N = 3$ and 4, J. Phys. A **34**, 8221 (2001).
- [52] J. G. Brankov, D. M. Danchev, and N. S. Tonchev, *The theory of critical phenomena in finite-size systems - scaling and quantum effects*, World Scientific, Singapore, 2000.
- [53] The heat-bath update of a single-site spin consists in the change $\mathbf{s}_x \rightarrow \mathbf{s}_x^{\text{new}}$ with probability $\sim \exp[-\mathcal{H}(\mathbf{s}_x^{\text{new}})/T]$ independent of the original spin \mathbf{s}_x , keeping the spins of the other sites fixed. Such an updating algorithm can be easily obtained by exploiting the fact that the Hamiltonian of the $O(N)$ vector model is linear with respect to each spin variable \mathbf{s}_x . A full sweep of the lattice is performed by first updating all spins at even sites and then all spins at odd sites of the cubic lattice.
- [54] The Metropolis update of a single spin \mathbf{s}_x consists in proposing a new spin $\mathbf{s}_x^{\text{new}} \neq \mathbf{s}_x$ using a generic distribution, for example by applying a random $O(N)$ rotation to \mathbf{s}_x . The proposed update is accepted with probability $\text{Min}[e^{\mathcal{H}(\mathbf{s}_x) - \mathcal{H}(\mathbf{s}_x^{\text{new}})}/T, 1]$. The Metropolis update becomes equivalent to the heat-bath one when a large number of trials at each site are performed.
- [55] N. V. Antonov and A. N. Vasilev, Critical dynamics as a field theory, Theor. Math. Phys. **60**, 671 (1984).
- [56] P. C. Hohenberg, B. I. Halperin, and S.-k. Ma, Calculation of Dynamic Critical Properties Using Wilson's Expansion Methods, Phys. Rev. Lett. **29**, 1548 (1972).
- [57] N. G. Van Kampen, *Stochastic Processes in Physics and Chemistry*, 3rd ed. (Elsevier, Amsterdam, 2007).
- [58] The integrated autocorrelation time of a given quantity Q is defined as $\tau \equiv \frac{1}{2} + \sum_{t=1}^{t=\infty} C(t)/C(0)$, where $C(t) = \langle (Q(t) - \langle Q \rangle)(Q(0) - \langle Q \rangle) \rangle$ is the autocorrelation function of Q and t is the discrete Monte Carlo time. Averages are taken at equilibrium. Estimates of the corresponding integrated autocorrelation time τ can be obtained by the binning method using the estimator $\tau = E^2/(2E_0^2)$, where E_0 is the naive error calculated without taking into account the autocorrelations, and E is the correct error, which can be computed using the blocking method [see H. Flyvbjerg and H. G. Petersen, Error estimates on averages of correlated data, J. Chem. Phys. **91**, 461 (1989)]. If b is the block length of the blocks

used to estimate E and n_b is the total number of available blocks, the statistical error $\Delta\tau$ is $\Delta\tau/\tau = \sqrt{2/n_b}$. This procedure leads to a systematic error of order τ/b [U. Wolff, Monte Carlo errors with less errors, Comput.

Phys. Commun. **156**, 143 (2004)]. In our case the ratio τ/b is much smaller than the statistical error, so that we can neglect it.